2018

Integration of routine QA data into mega-analysis may improve quality and sensitivity of multisite diffusion tensor imaging studies

P. Kochunov

E. W. Dickie

J. D. Viviano

J. Turner

P. B. Kingsley

See next page for additional authors

Authors
P. Kochunov, E. W. Dickie, J. D. Viviano, J. Turner, P. B. Kingsley, N. Jahanshad, P. M. Thompson, M. C. Ryan, A. K. Malhotra, A. N. Voineskos, and +6 additional authors

HHS Public Access

Author manuscript

Hum Brain Mapp. Author manuscript; available in PMC 2019 February 01.

Published in final edited form as:

Hum Brain Mapp. 2018 February ; 39(2): 1015–1023. doi:10.1002/hbm.23900.

Integration of routine QA data into mega-analysis may improve quality and sensitivity of multi-site diffusion tensor imaging studies

P Kochunov[1,*], **EW Dickie**[2,*], **JD Viviano**[2,*], **J Turner**[3], **PB Kingsley**[4], **N Jahanshad**[5], **PM Thompson**[5], **MC Ryan**[1], **E Fieremans**[6], **D Novikov**[6], **J Veraart**[6], **EL Hong**[1], **AK Malhotra**[4], **RW Buchanan**[1], **S Chavez**[2,7], and **AN Voineskos**[2,7]

[1]Maryland Psychiatric Research Center, Department of Psychiatry, University of Maryland School of Medicine, Baltimore

[2]Centre for Addiction and Mental Health, Toronto Canada

[3]Department of Psychology, Georgia State University, Atlanta, GA, USA

[4]Department of Radiology, North Shore University Hospital, Manhasset, NY, USA

[5]University of Southern California, California, USA

[6]Department of Radiology, New York University School of Medicine, New York, NY, USA

[7]Department of Psychiatry, University of Toronto, Canada

Abstract

Introduction—A novel mega-analytical approach that reduced methodological variance was evaluated using a multi-site diffusion tensor imaging (DTI) fractional anisotropy (FA) data by comparing white matter integrity in people with schizophrenia to controls. Methodological variance was reduced through regression of variance captured from quality assurance (QA) and by using Marchenko-Pastur Principal Component Analysis (MP-PCA) denoising.

Methods—N=192 (119patients/73controls) datasets were collected at three sites equipped with 3T MRI systems: GE MR750, GE HDx and Siemens Trio. DTI protocol included five b=0 and 60 diffusion-sensitized gradient directions (b=1000 s/mm^2). In-house DTI QA protocol data was acquired weekly using a uniform phantom; factor analysis was used to distil into two orthogonal QA factors related to: SNR and FA. They were used as site-specific covariates to perform mega-analytic data aggregation. The effect size of patient-control differences was compared to these reported by the Enhancing Neuro Imaging Genetics Meta Analysis (ENIGMA) consortium before and after regressing QA variance. Impact of MP-PCA filtering was evaluated likewise.

Results—QA-factors explained ~3–4% variance in the whole-brain average FA values per site. Regression of QA factors improved the effect size of schizophrenia on whole brain average FA values - from Cohen's d=0.53 to 0.57 - and improved the agreement between the regional pattern

Corresponding Author: (pkochunov@mprc.umaryland.edu), Maryland Psychiatric Research Center, Department of Psychiatry, University of Maryland School of Medicine, Baltimore, MD, USA, Phone: (410) 402-6110, Fax (410) 502-6778.

*KP, DEW and VJ equally contributed to this paper

of FA differences observed in this study vs. ENIGMA from r=0.54 to 0.70. Application of MP-PCA-denoising further improved the agreement to r=0.81.

Discussion—Regression of methodological variances captured by routine QA and advanced denoising that led to a better agreement with a large mega-analytic study.

INTRODUCTION

Lower integrity of cerebral white matter (WM), quantified as reduced fractional anisotropy (FA) of water diffusion measured from diffusion tensor imaging (DTI), is a consistent finding in schizophrenia (Alba-Ferrara and de Erausquin 2013; Ellison-Wright and Bullmore 2009; Friedman, et al. 2008; Glahn, et al. 2013; Kelly, et al. 2017; Kochunov and Hong 2014; Kubicki, et al. 2007; Nazeri, et al. 2012; Perez-Iglesias, et al. 2011; Phillips, et al. 2012; Wright, et al. 2015). FA deficits are hypothesized to be prominent in the associative WM fibers and responsible for neuropsychological deficits association with this disorder (Ellison-Wright and Bullmore 2009; Friedman, et al. 2008; Kochunov, et al. 2017; Kochunov, et al. 2016; Kubicki, et al. 2007; Nazeri, et al. 2012; Perez-Iglesias, et al. 2011). A challenge for evaluating regional WM deficits is the need for statistically powerful and representative samples that can be difficult to collect at a single site (Ioannidis 2014; Jahanshad, et al. 2013). Multi-site studies can collect larger and more representative samples but require pre-processing steps to address site-specific sources of methodological variance. The Enhancing Imaging Genetics Meta-Analysis (ENIGMA) consortium developed a multi-site homogenization approach for DTI data to address methodological biases in multi-site data (Jahanshad, et al. 2013). We sought to improve upon this approach, by evaluating two new steps aimed at addressing site-specific variances: a) regression of the site-specific variance captured through routine quality assurance (QA) program and b) Marchenko-Pastur Principal Component Analysis (MP-PCA) based noise reduction technique aimed at improving signal-to-noise ratio (SNR) and reporting potential artifacts that contribute to spatial non-uniformities of thermal noise. We tested these approaches in the data collected by the multi-center collaborative Social Processes Initiative In Neurobiology of the Schizophrenia(s) (SPINS) study.

We assessed the impact of regressing the site-specific methodological variance and advanced denoising approach by comparing the effect size of schizophrenia on regional FA values to those published by the largest meta-analytic analysis of regional FA deficits to date (N=1984/2391 patients/controls, thirty independent cohorts worldwide) performed by ENIGMA (Kelly, et al. 2017). The average effect size for regional FA values in ENIGMA was reported to be Cohen’s d=~0.25 (Kelly, et al. 2017). This suggested that a sample of N=250 patients/250 controls is required to detect such an effect size. The SPINS sample (N=192) is insufficiently powerful to reliably detect these regional differences. Therefore, the aim was to study the changes in the agreement in the pattern of regional difference between the SPINS and ENIGMA results. This study was focused on FA and did not explore other diffusion parameters (axial, radial, and mean diffusivities); FA was selected because it is the most commonly studied diffusion-metric in schizophrenia research, and is the metric most consistently altered between schizophrenia patients and matched controls (Kelly, et al. 2017).

METHODS

Subjects

The study was performed in N=192 participants (average age =32.7±10.1 years), including n=119 schizophrenia patients (age=33.6±13.3) and n=73 controls (age=31.2±10.2) collected at three sites (Table 1). Each site collected both patients and controls. Data for N=84 participants were collected at the Centre for Addiction and Mental Health, Toronto (CAMH); N=60 at the Maryland Psychiatric Research Center (MPRC), Baltimore; and N=47 at the Zucker-Hillside Hospital (ZHH), New York City. The demographic information is summarized in Table 1. Uniform clinical assessment and exclusion criteria were maintained across the three sites. The local Internal Review Boards approved the studies, and informed written consent was obtained from all participants. All participants had no current or past neurological conditions or major medical conditions. Patients were diagnosed with either schizophrenia or schizoaffective disorder as determined by the Structured Clinical Interview for DSM-IV or IV-TR (SCID). Controls had no Axis I psychiatric disorder as determined by the SCID. With the exception of nicotine, participants were excluded if they had DSM-IV substance abuse in the last 3 months or substance dependence within the past 6 months. Other exclusion criteria included diagnosis with uncontrolled hypertension, type 2 diabetes, heart disorders, or a major neurological event such as stroke or transient ischemic attack.

Diffusion Tensor Imaging (DTI)

Imaging data were collected using 3T MRI systems and multichannel head coils. A homogenized diffusion imaging protocol was developed for this study and implemented on each site using a consistent set of 60 gradient vectors (b=1000 s/mm^2) and five b=0 volumes. Details of the implementation of the protocol at each site are summarized in Table 2.

Image processing

DTI data from the three sites was processed using the ENIGMA-DTI analysis pipeline (http://enigma.ini.usc.edu/ongoing/dti-working-group/), which includes quality control and assurance QC/QA steps. One deviation from ENIGMA-DTI protocol was inclusion of the principal component analysis (PCA) based approach for automatic removal of noise-specific components, developed by Veraart and colleagues (Veraart, et al. 2016a; Veraart, et al. 2016b). The MP-PCA approach differs from traditional denoising approaches that improve SNR via spatial smoothing. Instead the MP-PCA approach quantifies the principal components that are fundamentally associated with thermal noise signal in magnitude MRI data. Noise contributes randomly to voxel-wise intensity values, but its contribution to the histogram of the eigenvalues of covariance matrix is deterministic (Veraart, et al. 2016b) and its eigenvalues are described by the Marchenko-Pastur (MP) distribution (Marchenko and Pastur 1967). The MP-PCA approach estimates the noise level and the number of significant signal components and regresses eigenvalues related to noise while not affecting the temporal or spatial domains of the data (Veraart, et al. 2016b). Quantification and regression of thermal noise can both enhance SNR and identify the spatial patterns of noise distribution within data (Veraart, et al. 2016b) (Figure S1, see supplement). The spatial distribution of thermal noise is independent of the underlying tissue type and therefore should have uniform

spatial distribution(Veraart, et al. 2016b). Spatial heterogeneity in the noise component may serve as an important QA parameter that provides information regarding the linearity and noise properties of the receiving elements of the RF coil as shown by artifacts observed in the data from one of the sites (Figure S1, see supplement). MP-PCA denoising was applied to raw DTI data using the default filter setting. Both raw and MP-PCA filtered data were processed using the ENIGMA-DTI pipeline.

Next, DTI data were corrected for motion and eddy current distortions using the eddy correction tool distributed as a part of FMRIB Software Library (FSL, “eddy_correct”) package (Smith, et al. 2006). FA maps were then generated by voxel-wise fitting of the local diffusion tensor. Next, individual FA maps were warped to an ENIGMA-DTI template and projected onto the ENIGMA-DTI skeleton that represents the middle of the tract of major white matter structures. ENIGMA-DTI per-tract average values were calculated by averaging values along tract regions of interest in both hemispheres. Overall average FA values were calculated by averaging values for the entire white matter skeleton, including the tract regions of interest and peripheral white matter. DTI data is sensitive to artifacts brought about by subject’s motion (Yendiki, et al. 2014). All data included in the analysis passed the ENIGMA-DTI QA/QC adopted from the report by Acheson and colleagues (Acheson, et al. 2017). The QA/QC steps included: visual inspection of raw and FA images, followed by calculating the frame-wise displacement and the average projection distance onto the skeleton.

DTI Quality Assurance

DTI QA was performed one to two times per week following each scanner reboot. The details of the QA protocol are discussed elsewhere (Chavez, et al. 2017). In short, the spherical (d=17.5 cm) agar-gel filled BIRN phantom (Biomedical Informatics Research Network) was used. The phantoms were stored in the scanner rooms to ensure temperature consistency. The QA protocol parameters matched imaging parameters used by the site. QA data were processed by a centralized automated QA pipeline (https://github.com/josephdviviano/qa-dti) (Chavez, et al. 2017). The average signal-to-noise ratio (SNR) measurements for b=0 and b=1000 s/mm^2 images and the average and standard deviation of the fractional anisotropy (FA) measurements showed trending correlations with whole-brain FA values in subjects. We included these measurements as potential explanatory variables for site-specific methodological variance.

The QA sessions were matched-in-time to the human imaging session. For each site we chose the closest QA session to the human imaging session (average time interval = 2.5 ± 1.1 days). Factor analysis was performed on the QA measures to distill orthogonal measurements of scanner stability. Factor analysis used principal components analysis (PCA) to extract linear composites of correlated variables with eigenvalues > 1. MP-PCA yielded eigenvalues describing the amount of variance among variables explained by a factor. A varimax rotation was used to remove collinearity (e.g., to orthogonalize individual eigenvectors). The factor analysis yielded factor loadings (correlations between a variable and a factor) and factor scores (a standardized score on each factor).

We compared the effect of the regression of the site-specific QA factor scores by comparing effect sizes observed in this study to these published by the ENIGMA-schizophrenia working group in the largest DTI study of patient-control differences in this disorder (www.enigma-viewer.org) (Kelly, et al. 2017). Specifically, we compared the regional FA differences observed here with ENIGMA's patient-control effect sizes across white matter regions in the brain (Table 5). The SPINS data were collected past the deadline for the submission to ENIGMA project and therefore can be treated as an independent replication sample. The results provide a definitive and independent assessment of white matter regions most vulnerable to schizophrenia.

Mega-Analysis

The ENIGMA-DTI mega-analysis algorithm was used to combine the data into a single population following regression of nuisance covariates and data homogenization. The goal of this analysis was to investigate the impact of the regression of QA-related variance on the overall effect size of schizophrenia on the whole-brain average and regional FA values. The ENIGMA-DTI mega-analysis uses two normalization steps: regression of covariates, per cohort, followed by the per-cohort inverse Gaussian normalization of data (Kochunov, et al. 2014). This produced the mega-analytic sample to quantify the significance of the global and regional differences in the FA values and calculating effect size (Cohen's *d*). Four analyses were conducted: the first used the standard per-site covariates (age, sex, age^2, age×sex, age^2×sex), followed by the standard and QA covariates (FA and SNR factors), followed by denoising and the standard covariates and the final analysis combined denoising with the standard and QA covariates.

RESULTS

Extraction of QA factors

Temporal stability plots for the factorized and raw QA measures are provided in supplement (Figure S2 and S3). Overall, all three system demonstrated a good stability (variance < 5%) across the 60 week period of data collection. Factor analysis in the SNR b=0, SNR b=1000, average FA and standard deviation FA measures produced two orthogonal factors that explained 94%, 92% and 97% of total variance in QA scores for the CAMH, MPRC and ZHH sites respectively (Table 3). The pattern of factor loading was similar for all three sites - with SNR and FA measurements loading on separate factors (Table 3).

Stability of QA factors

The scatter plot of QA factors over the week of scanning demonstrates that MPRC and ZHH sites experienced significant ($p<0.01$) linear changes in QA factors with time on one or both factors (Figure S2). The MPRC site showed significant increase in both SNR and QA factors ($r=0.37$ and 0.51, $p<0.02$). The ZHH site showed significant increase in SNR factor ($r=0.71$, $p<0.001$).

Correlation between QA factors and average FA values

The two orthogonal QA factors explained ~8.6% of the individual variance in the whole-brain FA values and this was significant for the MPRC site (11% variance explained,

p=0.047) with the correlation coefficients shown in Table 4. Only the FA factor showed consistent negative correlation with FA values at all three sites (r=−0.22, −0.06 and −0.24).

Effect of diagnosis before and after regression of QA factors

Patients showed lower average FA values than controls in each of three samples, after regression of age and sex effects (Figure 1, Table 5). This difference was only significant for MPRC and ZHH sites (Cohen's d=0.82 and 0.60, p=0.003 and 0.047 for MPRC and ZHH, respectively). The patient-control difference for CAMH sample were not significant (Cohen's d=0.25, p=0.23).

The pattern of regional d-values for each site was plotted versus effect sizes published by ENIGMA (Figure 1, Table 5). The correlation with ENIGMA pattern approached significance for MPRC sample (r=0.46, p=0.05). At CAMH and ZHH this correlation was not significant (r=0.0.5 and r=0.29, p>0.1).

Following inclusion of the QA factors Cohen's d values for CAMH improved from d=0.25 to d=0.31 but remained non-significant (p=0.16). The effect sizes for MPRC and ZHH were unchanged (Cohen's d= 0.78 and 0.62, p=0.004 and 0.048 for MPRC and ZHH, respectively). The correlation coefficients between per-site effect size and ENIGMA were improved (Figure 1). Changes were observed for all three sites: CAMH (r=0.05 to 0.25), MPRC (r=0.46 to 0.57) and ZHH (r=0.29 to 0.59). The correlation for both MPRC and ZHH became significant (p=~0.01). The correlation for CAMH remained non-significant (p=0.13).

Effect of diagnosis after MP-PCA-denoising and regression of QA factors

PCA denoising led to improvements in the effect size for whole-brain FA average for MPRC and ZHH sites (Cohen's d= 0.85 and 0.78, p=0.002 and 0.020 for MPRC and ZHH, respectively). The patient-control difference for CAMH sample remained non-significant (Cohen's d=0.22, p=0.25). Inclusion of QA factors did not cause a significant change (p>0.5) in effect size for MPRC and ZHH sites (Cohen's d= 0.86 and 0.76, p=0.002 and 0.020 for MPRC and ZHH, respectively).

The patterns of regional effect differences for each site were plotted versus effect sizes published by ENIGMA (Figure 1, Table 5). The MP-PCA denoising improved correlation with ENIGMA pattern (r=0.17, 0.50 and 0.41 for CAMH, MPRC and ZHH) this correlation.

Mega-analyses: effect of diagnosis before and after MP-PCA denoising and inclusion of QA factors

The mega-analyses of schizophrenia-related FA difference while accounting for age and sex demonstrated significantly reduced global FA values in patients compared to controls (Cohen's d=0.55, p=0.0006). MP-PCA denoising led to a slight increase in the effect size and significance (Cohen's d=0.57, p=0.0002).

Regional pattern of mega-analytical patient-control FA difference was significantly correlated with that reported by the ENIGMA schizophrenia analysis (r=0.54, p=0.02) (Figure 2). MP-PCA denoising improved this correlation (r=0.64, p=0.004). Inclusion of QA

factors in the regression of site-specific parameters slightly improved the patient control difference for global FA values (r=0.70, p=0.001). The best agreement was observed following MP-PCA and regression of QA factors (r=0.81, p=0.0001) (Figure 2, Table 5).

DISCUSSION

Many neuroimaging studies, such as the Social Processes Initiative in Neurobiology of Schizophrenia(s) (SPINS), use a multi-site design to collect statistically powerful datasets across diverse sites, MRI scanners, or platforms. DTI places a heavy demand on the stability of the MRI hardware; we therefore proposed a quantitative DTI QA protocol and data analysis to capture potential methodological variances (Chavez, et al. 2017). Quantitative metrics measured by this approach are sensitive to small drifts in hardware performance that do not produce detectable image artifacts (Chavez, et al. 2017; Wang, et al. 2011). We show that regression of this variance improves consistency of effect sizes across sites and makes the overall findings more agreeable with the findings of larger studies. In parallel, we show that a novel denoising technique that removes thermal noise from DTI images helps to improve the agreement of biological signal. Combining these two approaches produced the best outcome in terms of agreement between SPINS findings and those published in the largest cohort to date.

The two QA factors loaded on the SNR of the diffusion images and the average and standard deviation of FA values in the phantom. Longitudinal changes in SNR measurements may signify variability in the transmit/receive RF system, such as variance in the coil elements/pre-amplifiers/amplifiers and other system instabilities. In a noise-free, uniform agar-gel phantom, water is expected to diffuse freely in all directions, leading to zero average FA values (Friedman, et al. 2006a; Friedman, et al. 2006b). The measurement of FA from an agar-gel phantom simultaneously captures the effect of noise, gradient instability, and gradient nonlinearity, as suggested by Wang and colleagues (Chavez, et al. 2017; Wang, et al. 2011).

Plots of factorized QA metrics over the two-year period of data collection showed that all three sites demonstrated good stability (<5% variance) (Chavez, et al. 2017). However, the time-related trends of factorized QA metrics differed across sites. The SNR factor showed significant negative correlation with time for CAMH and a positive correlation for MPRC and ZHH (Figure 1). The FA factor showed significant positive correlation with time for MPRC and no changes for two other sites. Such deviations are expected for a multisite study, as system performances for different vendors/models are rarely consistent across sites or time.

Inclusion of the methodological variance captured from QA into the data analysis improved the agreement between the effect sizes among global and regional effect values observed in SPINS sample and those published by ENIGMA. Two orthogonal QA factors explained between 7.5 and 11.5% of the intersubject variance per site. Both QA factors contributed to explaining methodological variances observed in human FA values; the effect of removal of this variance was site-specific and led to both higher and lower effect sizes. For instance, for all three sites, higher average FA values in the FBIRN phantom were associated with lower

FA values in human subjects scanned the same week. Such an erroneous variance may both increase and decrease the observed effect sizes per site. The non-zero average FA values in the phantom is the consequence of mismatches between the recorded gradient direction/b-value and these executed by the gradient system (Wang, et al. 2011). Deviations between the expected and the executed gradients, as well contamination by noise may cause both reduced and increased voxel-wise FA values in human participants by introducing fit error into the DTI model.

PCA denoising further improved agreement. DTI is an SNR-limited technique but increasing SNR with longer scan time can lead to a diminishing return due to subject motion and other physiological artifacts (Hansen, et al. 2013; Hansen, et al. 2016; Poot, et al. 2010; Veraart, et al. 2016b). Spatial smoothing such as Gaussian kernel filtering are not appropriate for improving SNR in DTI as spatial averaging of the signal from nearby voxels may interfere with the fitting of the diffusion tensor model (Molloy, et al. 2014; Triantafyllou, et al. 2006). Instead, advanced denoising techniques can improve SNR characteristics and fidelity of DTI-derived parameters by taking advantage of the spatial and temporal redundancy of the data. We used a MP-PCA-based denoising technique to reduce signal fluctuations rooted in thermal noise and hence increase the SNR without altering the spatial resolution (Figure S2). The thermal noise-selective nature is based on data redundancy in the MP-PCA domain using universal properties of the eigenspectrum of random covariance matrices (Veraart, et al. 2016b). The MP-PCA-denoising brought the biggest improvements in the SNR-limited ZHH data that was collected with an older MRI scanner (Figure S1). It also revealed regional inhomogeneity of the noise structure in that dataset, which may be used as an important characteristic for future QA design. On the other hand, MP-PCA denoising only showed minor changes in the MPRC dataset that was collected with the newest MRI scanner and a 32-channel coil (Figure S2). The changes in CAMH dataset were intermediate.

In summary, regression of site-specific QA factors and application of MP-PCA-based denoising produced improved correlation between regional patterns of FA deficits observed in SPINS subjects and these published by the largest-to-date meta-analysis study (N=1,984/2,391 patients/controls). The observed improvements were modest but showed the outcomes of the SPINS study now more faithfully approximate the expected results. Our experiment demonstrates the importance of well-powered samples in solving the problems of reproducibility in biomedical research. We used ENIGMA regional effect sizes as the “gold standard” to study the impact of data homogenization steps. The effect of diagnosis on FA values varied among the three sites due to differences in sample and methodological variance. The ZHH and MPRC samples showed higher effect sizes than ENIGMA, while CAMH sample showed only modest effect size. The mega-analytic aggregation with regression of methodological and noise-related variances improved the agreement between SPINS and ENIGMA findings. The SPINS sample was insufficiently powerful to detect regional findings and regression of methodological variance reduced significance of some of the regional effects despite providing a better agreement with ENIGMA. Therefore, the comparison with ENIGMA was used to show that smaller samples can achieve the expected patter of effect without achieving statistical significance.

Future directions should focus on quantifying regional site-specific QA variance. Present assessment was aimed at overall quantification of the site-specific variance. The spatial maps of the noise derived from the MP-PCA approach indicated that methodological variance was regionally variable presumably due to non-linearity in RF-receiving elements of the coil or reconstruction algorithms or other scanner hardware or software related problems. Our observations should stimulate development of QA phantoms that approximate both the geometry of a typical human head and the non-anisotropy of human white matter for deriving regional QA indices.

CONCLUSION

Regressing methodological variances captured via a DTI-specific QA program and reducing signal variances using an advanced denoising approach made the outcomes of a relatively smaller multi-center study more reproducible as judged by comparison with the largest meta-analyses to date.

Supplementary Material

Refer to Web version on PubMed Central for supplementary material.

Acknowledgments

Support was received from NIH grants 1/3R01MH102324, 2/3R01MH102324, 3/3R01MH102324, R01EB015611. This work was also supported in part by the NIH Big Data to Knowledge (BD2K) Initiative (U54 EB020403).

References

Acheson A, Wijtenburg S, Rowland L, Winkler A, Mathias CW, Hong L, Jahanshad N, Patel B, Thompson P, McGuire S, Sherman P, Kochunov P, Dougherty DD. Reproducibility of tract-based white matter microstructural measures using the ENIGMA-DTI protocol. Genes Brain Behav. 2017; 7(2):10. 1002/brb3.615.

Alba-Ferrara LM, de Erausquin GA. What does anisotropy measure? Insights from increased and decreased anisotropy in selective fiber tracts in schizophrenia. Front Integr Neurosci. 2013; 7:9. [PubMed: 23483798]

Chavez S, Viviano J, Zamyadi M, Kingsley P, Kochunov P, Strothers S, Voineskos A. A novel DTI-QA tool: automated metric extraction exploiting the sphericity of an agar filled phantom. Magnetic Resonance Imaging. 2017 In Press.

Ellison-Wright I, Bullmore E. Meta-analysis of diffusion tensor imaging studies in schizophrenia. Schizophr Res. 2009; 108(1–3):3–10. [PubMed: 19128945]

Friedman JI, Tang C, Carpenter D, Buchsbaum M, Schmeidler J, Flanagan L, Golembo S, Kanellopoulou I, Ng J, Hof PR, Harvey PD, Tsopelas ND, Stewart D, Davis KL. Diffusion tensor imaging findings in first-episode and chronic schizophrenia patients. Am J Psychiatry. 2008; 165(8): 1024–32. [PubMed: 18558643]

Friedman L, Glover GH, Krenz D, Magnotta V. Reducing inter-scanner variability of activation in a multicenter fMRI study: Role of smoothness equalization. Neuroimage. 2006a; 32(4):1656–1668. [PubMed: 16875843]

Friedman L, Glover GH, The FC. Reducing interscanner variability of activation in a multicenter fMRI study: Controlling for signal-to-fluctuation-noise-ratio (SFNR) differences. Neuroimage. 2006b; 33(2):471–481. [PubMed: 16952468]

Glahn DC, Kent JW Jr, Sprooten E, Diego VP, Winkler AM, Curran JE, McKay DR, Knowles EE, Carless MA, Goring HH, Dyer TD, Olvera RL, Fox PT, Almasy L, Charlesworth J, Kochunov P,

Duggirala R, Blangero J. Genetic basis of neurocognitive decline and reduced white-matter integrity in normal human brain aging. Proc Natl Acad Sci U S A. 2013; 110(47):19006–11. [PubMed: 24191011]

Hansen B, Lund TE, Sangill R, Jespersen SN. Experimentally and computationally fast method for estimation of a mean kurtosis. Magn Reson Med. 2013; 69(6):1754–1760. [PubMed: 23589312]

Hansen B, Lund TE, Sangill R, Stubbe E, Finsterbusch J, Jespersen SN. Experimental considerations for fast kurtosis imaging. Magn Reson Med. 2016; 76:1455–1468. [PubMed: 26608731]

Ioannidis JPA. How to Make More Published Research True. PLoS Medicine. 2014; 11(10):e1001747. [PubMed: 25334033]

Jahanshad N, Kochunov P, Sprooten E, Mandl RC, Nichols TE, Almassy L, Blangero J, Brouwer RM, Curran JE, de Zubicaray GI, Duggirala R, Fox PT, Hong LE, Landman BA, Martin NG, McMahon KL, Medland SE, Mitchell BD, Olvera RL, Peterson CP, Starr JM, Sussmann JE, Toga AW, Wardlaw JM, Wright MJ, Hulshoff Pol HE, Bastin ME, McIntosh AM, Deary IJ, Thompson PM, Glahn DC. Multi-site genetic analysis of diffusion images and voxelwise heritability analysis: A pilot project of the ENIGMA-DTI working group. Neuroimage. 2013; pii: S1053-8119(13)00408-4. doi: 10.1016/j.neuroimage.2013.04.061

Kelly S, Jahanshad N, Zalesky A, Kochunov P, Hibar D, Chen J, Agartz I, Alloza C, Andreassen O, Arango C, Banaj N, Bouix S, Bousman C, Brouwer R, Bruggemann J, Bustillo J, Cahn W, Calhoun V, Cannon D, Carr V, Catts S, Chen J, Chen X, Chiapponi C, Cho K, Ciullo V, Corvin A, Crespo-Facorro B, Cropley V, De Rossi P, Diaz-Caneja C, Dickie E, Doan N, Fan F, Faskowitz J, Fatouros-Bergman H, Flyckt L, Ford J, Fouche J, Fukunaga M, Gill M, Glahn D, Gollub R, Goudzwaard E, Guo H, Gur R, Gur R, Hashimoto R, Hatton S, Henskens F, Hickie I, Hong L, Horacek J, Howells F, Hulshoff Pol H, Hyde C, Isaev D, Whitford T, Jablensky A, Jansen P, Janssen J, Jonsson E, Kahn R, Kikinis R, Liu K, Klauser P, Knöchel M, Kubicki M, Kwon J, Lagopoulos J, Langen C, Lawrie S, Lenroot R, Lim K, López-Jaramillo C, Lyall A, Magnotta V, Mandl R, Mathalon D, McCarley R, McCarthy-Jones S, McDonald C, McEwen S, Mcintosh A, Melicher T, Mesholam-Gately R, Michie P, Mowry B, Mueller B, Newell D, O'Donnell P, Oertel V, Oestreich L, Paciga S, Pantelis C, Pasternak O, Pearlson G, Pereira A, Pineda J, Piras F, Piras F, Potkin S, Preda A, Rasser A, Roalf D, Roiz-Santiañez R, Pellicano G, Roos A, Rotenberg D, Satterthwaite T, Savadjiev P, Schall U, Scott R, Seal M, Seidman L, Weickert C, Shenton M, Spalletta G, Spaniel F, Sprooten E, Stäblein M, Stein D, Sundram S, Tan Y, Tan S, Tang S, Temmingh H, Tønnesen S, Tordesillas-Gutierrez D, Vaidya J, Haren D, Vargas C, Vecchio D, Velakoulis D, Voineskos A, Voyvodic J, Wang Z, Wang P, Wei D, Weickert T, Westlye L, Whalley H, White T, Wojcik J, Xiang H, Xie Z, Yamamori H, Yang F, Yao N, Zhang D, Zhao J, van Erp T, Turner J, Ehrlich S, Jung L, Thompson P, Donohue G. Widespread white matter microstructural differences in schizophrenia across 4,375 individuals: results from the ENIGMA Schizophrenia DTI Working Group. Mol Psychiatry. 2017 In Press.

Kochunov P, Coyle T, Rowland L, Jahanshad N, Thompson P, Kelly S, Du X, Sampath H, Bruce H, Chiappelli J, Ryan M, Fisseha F, Savransky A, Adhikari B, Chen C, Paciga S, Whelan C, Xie Z, Hyde C, Chen X, Schubert C, O'Donnell P, LEH. White Matter and Core Cognitive Deficits in Schizophrenia. JAMA Psychiatry. 2017 In Press.

Kochunov P, Ganjgahi H, Winkler A, Kelly S, Shukla DK, Du X, Jahanshad N, Rowland L, Sampath H, Patel B, O'Donnell P, Xie Z, Paciga SA, Schubert CR, Chen J, Zhang G, Thompson PM, Nichols TE, Hong LE. Heterochronicity of white matter development and aging explains regional patient control differences in schizophrenia. Hum Brain Mapp. 2016

Kochunov P, Hong LE. Neurodevelopmental and neurodegenerative models of schizophrenia: white matter at the center stage. Schizophr Bull. 2014; 40(4):721–8. [PubMed: 24870447]

Kochunov P, Jahanshad N, Sprooten E, Nichols TE, Mandl RC, Almasy L, Booth T, Brouwer RM, Curran JE, de Zubicaray GI, Dimitrova R, Duggirala R, Fox PT, Elliot Hong L, Landman BA, Lemaitre H, Lopez LM, Martin NG, McMahon KL, Mitchell BD, Olvera RL, Peterson CP, Starr JM, Sussmann JE, Toga AW, Wardlaw JM, Wright MJ, Wright SN, Bastin ME, McIntosh AM, Boomsma DI, Kahn RS, den Braber A, de Geus EJ, Deary IJ, Hulshoff Pol HE, Williamson DE, Blangero J, van't Ent D, Thompson PM, Glahn DC. Multi-site study of additive genetic effects on fractional anisotropy of cerebral white matter: Comparing meta and megaanalytical approaches for data pooling. Neuroimage. 2014; 95C:136–150.

Kubicki M, McCarley R, Westin CF, Park HJ, Maier S, Kikinis R, Jolesz FA, Shenton ME. A review of diffusion tensor imaging studies in schizophrenia. J Psychiatr Res. 2007; 41(1–2):15–30. [PubMed: 16023676]

Marchenko VA, Pastur LA. Distribution of eigenvalues for some sets of random matrices. Matematicheskii Sbornik. 1967; 114(4):507–536.

Molloy EK, Meyerand ME, Birn RM. The influence of spatial resolution and smoothing on the detectability of resting-state and task fMRI. NeuroImage. 2014; 86:221–30. [PubMed: 24021836]

Nazeri A, Mallar Chakravarty M, Felsky D, Lobaugh NJ, Rajji TK, Mulsant BH, Voineskos AN. Alterations of Superficial White Matter in Schizophrenia and Relationship to Cognitive Performance. Neuropsychopharmacology. 2012

Perez-Iglesias R, Tordesillas-Gutierrez D, McGuire PK, Barker GJ, Roiz-Santianez R, Mata I, de Lucas EM, Rodriguez-Sanchez JM, Ayesa-Arriola R, Vazquez-Barquero JL, Crespo-Facorro B. White matter integrity and cognitive impairment in first-episode psychosis. Am J Psychiatry. 2011; 167(4):451–8.

Phillips KA, Rogers J, Barrett EA, Glahn DC, Kochunov P. Genetic contributions to the midsagittal area of the corpus callosum. Twin Res Hum Genet. 2012; 15(3):315–23. [PubMed: 22856367]

Poot DHJ, den Dekker AJ, Achten E, Verhoye M, Sijbers J. Optimal experimental design for diffusion kurtosis imaging. Med Imaging, IEEE Trans. 2010; 29(3):819–829.

Smith SM, Jenkinson M, Johansen-Berg H, Rueckert D, Nichols TE, Mackay CE, Watkins KE, Ciccarelli O, Cader MZ, Matthews PM, Behrens TE. Tract-based spatial statistics: Voxelwise analysis of multi-subject diffusion data. Neuroimage. 2006; 31(4):1487–505. [PubMed: 16624579]

Triantafyllou C, Hoge RD, Wald LL. Effect of spatial smoothing on physiological noise in high-resolution fMRI. NeuroImage. 2006; 32(2):551–557. [PubMed: 16815038]

Veraart J, Fieremans E, Novikov DS. Diffusion MRI noise mapping using random matrix theory. Magn Reson Med. 2016a; 76:1582–1593. [PubMed: 26599599]

Veraart J, Novikov DS, Christiaens D, Ades-Aron B, Sijbers J, Fieremans E. Denoising of diffusion MRI using random matrix theory. NeuroImage. 2016b; 142:394–406. [PubMed: 27523449]

Wang ZJ, Seo Y, Chia JM, Rollins NK. A quality assurance protocol for diffusion tensor imaging using the head phantom from American College of Radiology. Medical Physics. 2011; 38(7):4415–4421. [PubMed: 21859042]

Wright SN, Hong LE, Winkler AM, Chiappelli J, Nugent K, Muellerklein F, Du X, Rowland LM, Wang DJ, Kochunov P. Perfusion shift from white to gray matter may account for processing speed deficits in schizophrenia. Hum Brain Mapp. 2015

Yendiki A, Koldewyn K, Kakunoori S, Kanwisher N, Fischl B. Spurious group differences due to head motion in a diffusion MRI study. Neuroimage. 2014; 88C:79–90.

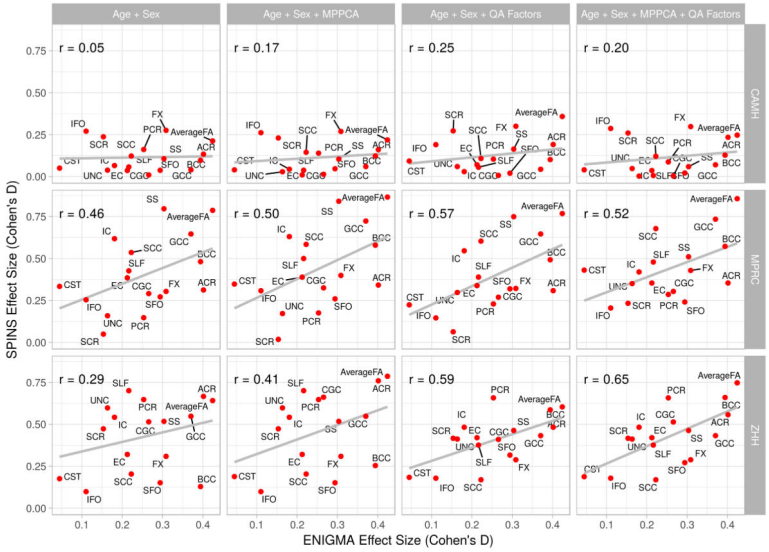

Figure 1.

Correlation between regional effects of diagnosis (Cohen's d-values) for each of the three sites versus ENIGMA effect sizes plotted after regression of age and sex, QA-factors and MP-PCA denoising.

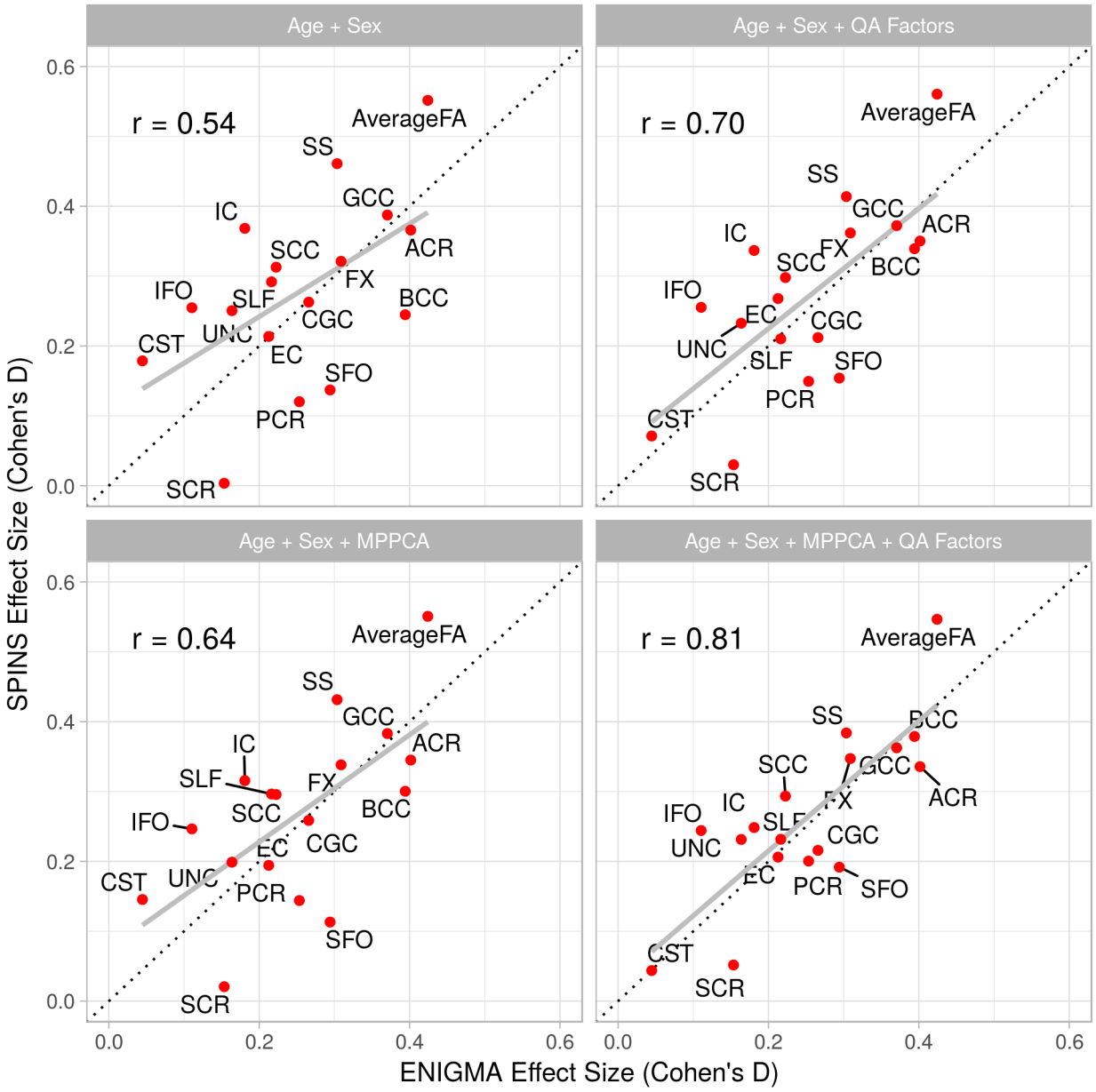

Figure 2.

Comparison of regional mega-analytic effect sizes following inclusion of the QA factors and MP-PCA denoising.

Table 1

Subject demographics for the Centre for Addiction and Mental Health (CAMH), Maryland Psychiatric Research Center (MPRC) and Zucker Hillside Hospital (ZHH) sites. Severity of psychiatric symptoms was ascertained using the Brief Psychiatric Rating Scale (BPRS). Antipsychotic medication dose is provided in the chlorpromazine equivalent dose (mg/day). The severity of tobacco dependence was ascertained using the Fagerstrom Test for Nicotine Dependence (FTDN).

	CAMH		**MPRC**		**ZHH**	
	Patients (34M/17F)	**Controls (17M/16F)**	**Patients (36M/8F)**	**Controls (13M/8F)**	**Patients (15M/14F)**	**Controls (9M/9F)**
Average Age, Range (years)	28.9±9.3 18–50	25.9±6.7 18–47	37.9±10.5 19–55	38.5±11.1 20–55	36.6±8.8 23–55	32.6±9.4 20–50
BPRS (total)	29.8±6.8	N/A	33.5±8.8	N/A	30.9±9.2	N/A
Age-of-Onset (years)	21.3±5.6	N/A	20.3±6.3	N/A	18.9±5.9	N/A
Illness Duration (years)	8.9±7.2	N/A	15.4±11.2	N/A	16.4±11.3	N/A
Education (year)	13.1±7.2	15.5±2.0	13.1±2.8	15.7±1.9	13.4±3.2	15.2±2.2
IQ	108.1±16.2	116.5±8.4	100.1±20.6	115.5±9.6	96.3±20.6	107.5±14.6
Handedness (% right)	84%	91%	86%	91%	84%	72%
Medication Dose (CPZ)	376.3±270.1		543.3±387.4		471.3±426.5	
Current Smokers	31%	18%	39%	35%	41%	12%
FTND	3.6±3.0					

Table 2

DTI sequence parameters for Centre for Addiction and Mental Health (CAMH), Maryland Psychiatric Research Center (MPRC) and Zucker Hillside Hospital (ZHH) sites. Partial k-space acceleration techniques, Array Spatial Sensitivity Encoding Technique (Asset) and Generalized Autocalibrating Partially Parallel Acquisitions (GRAPPA) were used on GE and Siemens scanners, respectively, to reduce effective TE and TE by undersampling k-space along the phase encoding direction. A twice refocused spin-echo EPI sequence was used on the GE scanners to improve spatial distortions. A refocused mono-polar EPI sequence was used on the Siemens scanner to improve SNR.

	CAMH	**MPRC**	**ZHH**
MRI system	GE MR750 Discovery	Siemens Trio	GE HDx
Year of Installation	2010	2011	2004
Head Coil	8-channel	12-channel	8-channel
Acceleration	Asset=2	GRAPPA=2	Asset=2
Echo Time (ms)	88	85	88
Repetition Time (ms)	8800	8800	17000
Flip Angle (degrees)	90/180/180	90/180	90/180/180
FOV (mm)	256	256	256
In-plane resolution (mm)	2.0×2.0	2.0×2.0	2.0×2.0
Slice Thickness (mm)	2.0	2.0	2.0
Number of Slices	66	66	66

Table 3

Factor analyses using principal component extraction and orthogonalization were performed on QA data collected at the three sites.

	SNR Factor Loading	FA Factor loading
CAMH		
SNRb0	.98	−0.06
SNRdwi	.97	−0.05
Average FA	−0.64	.72
StdDev FA	.35	.98
MPRC		
SNRb0	.96	−0.12
SNRdwi	.97	−0.06
Average FA	−0.10	.93
StdDev FA	.05	.93
ZHH		
SNRb0	.98	−.17
SNRdwi	.97	−.14
Average FA	−.89	.41
StdDev FA	−.18	.98

Table 4

Pearson correlation coefficients between average FA values and two orthogonal QA factors and percent variance in average FA explained by two factors based on linear regression analysis.

Site	SNR Factor	FA Factor	% Variance explained (p-value)
CAMH	0.03	−0.22	11.0 (p=0.047)
MPRC	0.09	−0.04	7.5 (p=0.11)
ZHH	−0.08	−0.24	11.5 (p=0.16)

Hum Brain Mapp. Author manuscript; available in PMC 2019 February 01.

Table 5

Effect size (Cohen's d) of patient-control differences for whole-brain and regional FA measurements. First column shows ENIGMA effects sizes (Kelly, et al. 2017). SPIN-Mega analysis results are shown after correction for covariates, in parenthesis, including age, sex and QA factors (2nd and 3rd column) and following MP-PCA denoising and correction for covariates

Tract	ENIGMA Cohen's d (p-value) *	Mega Analysis(age and sex) Cohen's d (p-value)	Mega Analysis (age, sex and qa factors) Cohen's d (p-value)	MP-PCA Mega Analysis (age and sex) Cohen's d (p-value)	MP-PCA Mega Analysis (age, sex, qa factors) Cohen's d (p-value	Fiber Type	Connections
Whole-Brain Average	0.42 (4×10-24)	0.55 (0.0006)	0.56 (0.0005)	0.57 (0.0002)	0.55 (0.0002)		
Regional							
Genu (GCC)	0.37 (1×10-18)	0.39 (0.015)	0.37 (0.0195)	0.38 (0.01)	0.36 (0.02)	C	Cerebral Hemispheres
Body (BCC)	0.39 (3×10-18)	0.24 (0.12)	0.34 (0.0330)	0.30 (0.04)	0.37 (0.01)	C	Cerebral Hemispheres
Splenium (SCC)	0.22 (4×10-6)	0.31 (0.049)	0.29 (0.0608)	0.29 (0.04)	0.29 (0.04)	C	Cerebral Hemispheres
Anterior CR (ACR)	0.40 (9×10-19)	0.37 (0.021)	0.35 (0.0278)	0.35 (0.02)	0.34 (0.02)	A/P/C	Cortical/Subcortical
Superior CR (SCR)	0.15 (7×10-6)	0.00 (0.98)	0.03 (0.8493)	0.02 (0.9)	0.05 (0.8)	A/P/C	Cortical/Subcortical
Posterior CR (PCR)	0.25 (2×10-12)	0.12 (0.44)	0.15 (0.3455)	0.14 (0.36)	0.20 (0.18)	A/P/C	Cortical/Subcortical
Cingulum (CGC)	0.27 (3×10-9)	0.26 (0.09)	0.22 (0.1812)	0.26 (0.08)	0.36 (0.02)	A	Cingulate Gyrus/Hippocampus
Cortico-spinal tract (CST)	0.04 (0.3)	0.18 (0.25)	0.07 (0.6526)	0.14 (0.44)	0.04 (0.98)	P	Cortical/Spinal Cord
External Capsule (EC)	0.21 (1×10-7)	0.21 (0.17)	0.26 (0.0915)	0.19 (0.17)	0.20 (0.12)	A	Frontal/Temporal/Occipital
Internal Capsule (IC)	0.18 (2×10-5)	0.37 (0.020)	0.33 (0.0343)	0.32 (0.02)	0.20 (0.12)	P	Subcortical/Brainstem/Cortex
Fornix (FX)	0.31 (7×10-12)	0.32 (0.043)	0.36 (0.0230)	0.33 (0.03)	0.34 (0.02)	P/C	Hippocampus/Thalamus
Inferior Fronto-Occipital (IFO)	0.11 (0.003)	0.25 (0.10)	0.25 (0.1075)	0.25 (0.10)	0.24 (0.11)	A	Frontal/Temporal/Occipital
Superior Fronto-Occipital (SFO)	0.29 (4×10-8)	0.14 (0.38)	0.16 (0.3305)	0.11 (0.35)	0.11 (0.35)	A	Frontal/Parietal/Occipital
Superior Longitudinal Fasciculus (SLF)	0.22 (6×10-8)	0.29 (0.06)	0.21 (0.1848)	0.29 (0.04)	0.23 (0.11)	A	Frontal/Temporal/Occipital
Sagittal Stratum (SS)	0.30 (5×10-14)	0.46 (0.004)	0.41 (0.0095)	0.43 (0.004)	0.38 (0.01)	A/P	Subcortical/Temporal/Occipital
Uncinate Fasciculus (UNC)	0.16 (9×10-7)	0.25 (0.12)	0.23 (0.1424)	0.20 (0.18)	0.20 (0.18)	P	Hypothalamus/Orbitofrontal